K-Shell Core-Electron Excitations in Electronic Stopping of Protons in Water from First Principles

Yi Yao, Dillon C. Yost, and Yosuke Kanai*
Department of Chemistry, University of North Carolina at Chapel Hill, North Carolina 27599, USA

(Received 12 February 2019; revised manuscript received 17 April 2019; published 5 August 2019)

Understanding the role of core-electron excitation in liquid water under proton irradiation has become important due to the growing use of proton beams in radiation oncology. Using a first-principles, nonequilibrium simulation approach based on real-time, time-dependent density functional theory, we determine the electronic stopping power, the velocity-dependent energy transfer rate from irradiating ions to electrons. The electronic stopping power curve agrees quantitatively with experimental data over the velocity range available. At the same time, significant differences are observed between our first-principles result and commonly used perturbation theoretic models. Excitations of the water molecules' oxygen core electrons are a crucial factor in determining the electronic stopping power curve beyond its maximum. The core-electron contribution is responsible for as much as one third of the stopping power at the high proton velocity of 8.0 a.u. (1.6 MeV). *K*-shell core-electron excitations not only provide an additional channel for the energy transfer—they also significantly influence the valence electron excitations. In the excitation process, generated holes remain highly localized within a few angstroms around the irradiating proton path, whereas electrons are excited away from the path. In spite of their great contribution to the stopping power, *K*-shell electrons play a rather minor role in terms of the excitation density; only 1% of the hole population composes *K*-shell holes, even at the high proton velocity of 8.0 a.u. The excitation behavior revealed is distinctly different from that of photon-based ionizing radiation such as x or γ rays.

DOI: 10.1103/PhysRevLett.123.066401

When a highly energetic ion travels through and interacts with matter, its kinetic energy is transferred into the target material's electronic and nuclear subsystems. This energy loss of the projectile ion can arise from both elastic collisions with nuclei (nuclear stopping) and inelastic scattering events (electronic stopping). When the particle's kinetic energy is sufficiently large (on the order of $\sim$10 keV per nucleon), the major contribution to the energy transfer constitutes electronic stopping, wherein the projectile ion induces massive electronic excitations in the target matter [1,2]. This electronic stopping phenomenon is at the heart of emerging ion beam cancer therapies. The use of proton beam radiation over more conventional radiation based on x- or γ-ray photons is often considered more effective because of the ion's distinct spatial energy deposition profile with a very sharp peak [3,4]. By calibrating the initial kinetic energy of the protons, this energy deposition peak can be tuned to coincide with the location of the tumor. This energy deposition profile is largely determined by the electronic stopping power, which measures the rate of energy transfer from the charged particle to electrons in matter per unit distance of the energetic particle's movement [1,5–7]. The stopping power is a continuous function of the particle velocity, and the velocities near the maximum of the stopping power are responsible for the formation of the sharp energy deposition peak for ions like protons. Because liquid water makes up the majority of matter in human cells, various models have been developed for the electronic stopping power in liquid water over the years [8–16], including our earlier first-principles theory result [17–18]. At the same time, only limited experimental measurements exist near the stopping power maximum, and various theoretical models are currently used with empirically fitted parameters. Furthermore, unraveling the details of the excitation behavior in the electronic stopping process has become important. Proton radiation is generally considered to be similar to other types of ionizing radiation like x- or γ-ray photons, which undergo Compton scattering and also core-electron excitation. However, the extent to which proton radiation excites valence and core electrons is not understood. Indeed, this is complicated by the fact that the ratio of valence to core-electron excitations depends on the irradiating proton velocity. In radiation oncology, an empirical factor such as relative biological effectiveness is used to take into account differences between the proton radiation and x-ray photon radiation for convenience, but many now call for a better mechanistic understanding of the radiation at the molecular level [19]. In this Letter, we discuss the role of *K*-shell core-electron excitations in liquid water under proton irradiation by accurately determining the electronic stopping power and simulating the quantum dynamics of electronic excitations from first principles.

We apply our recently developed nonequilibrium dynamics simulation approach based on real-time, time-dependent density functional theory (RTTDDFT) [17,18,20–23] to simulate the nonperturbative response of the electronic system to a fast-moving projectile proton. In this approach, the electronic stopping power can be obtained from the rate of electronic energy change at different projectile proton velocities, as discussed in our earlier work [21,24]. We use our implementation of RTTDDFT based on a plane wave–pseudopotential (PW-PP) formalism [20,25] in the QBOX/QB@LL code [26,27]. Simulating the $1s$ core (i.e., K-shell) electron excitations of oxygen atoms in this Letter requires us to go beyond several standard approximations typically used in the PW-PP formalism. The oxygen and hydrogen atoms in liquid water are described by all-electron pseudopotentials that are generated using the optimized norm-conserving Vanderbilt scheme [28,29], for which multiple projectors are used for the explicit treatment of the $1s$ electrons of oxygen atoms in the simulation. The validity of the all-electron pseudopotentials was checked by calculating the core-level optical excitation spectrum of a single water molecule, as shown in the Supplemental Material [30]. Unlike previous RTTDDFT studies of electronic stopping in which pseudopotentials are used for the projectile proton [17,18], here we use a bare Coulomb potential for representing the proton because an accurate description of the K-shell core excitations is necessary, especially for large proton velocities (see the Supplemental Material [30] for details). Consequently, the use of a plane wave kinetic energy cutoff of up to 250 Ry for expanding the Kohn-Sham wave functions was required, and an extrapolation was used for calculating the stopping power at high velocities (see the Supplemental Material [30] for details). We employed the Perdew-Burke-Ernzerhof generalized gradient approximation (GGA) approximation [34] for the exchange-correlation potential because we found that the use of the more advanced strongly constrained and appropriately normed meta-GGA does not change the results [35–37] (see Fig. S7 in the Supplemental Material [30]). The liquid water structure was generated by taking a snapshot after preforming a 10 ns classical molecular dynamics simulation at 300 K with extended simple point charge force field [38]. Our simulation cell contains 38 water molecules with periodic boundary conditions (8 Å × 8 Å × 17.73 Å), and the projectile proton travels in the $+z$ direction. This simulation was compared to a larger simulation cell with 170 water molecules (12 Å × 12 Å × 35.45 Å), and no appreciable finite size errors were found. In order to determine electronic stopping power accurately using the nonequilibrium simulation approach, an ensemble average of projectile proton trajectories is necessary [23]. Sixty-four proton projectile trajectories (paths) were sampled evenly on a grid dividing the cross section of the xy simulation cell plane. In total, 64 independent RTTDDFT simulations were performed for each velocity. The convergence of this sampling was confirmed by comparison with a more extensive sampling that includes 256 paths. Albeit computationally expensive, this trajectory sampling ensures that the ensemble average contains projectile proton trajectories that cover a wide range of impact parameters with respect to the atoms in the target matter, which is especially important when core electrons are excited [23,39]. The error bars on the stopping power reported here are the standard error of the mean calculated based on these 64 paths. Because the K-shell core-electron excitation is found to be important in the high velocity regime, we also verified that close or small impact parameters are accurately sampled. These technical, but important, details are discussed in the Supplemental Material [30], in addition to comparisons with our earlier work [18], which did not consider core-electron effects.

The calculated stopping power as a function of the proton velocity ranging from 0.5 to 8 a.u. (corresponding to the kinetic energy of 6.2 keV–1.6 MeV) is compared to the available experimental stopping power data [40,41] and to the so-called stopping and range of ions in matter (SRIM) [16] model in Fig. 1. The only experimental data available in this velocity range are the measurements by Shimizu and co-workers [40,41]. We note, for completeness, that the reliability of this measurement has been questioned on the basis of the Bethe model [42]. The SRIM model is based on extending the Lindhard-Scharff-Schiott theory [43] with inputs from available experiments, and it is widely used as a standard reference. Though there is no reported experimental data for velocities less than 3.5 a.u. for liquid water, the SRIM result relies on existing experimental data of solid water (ice) to estimate the stopping power of liquid

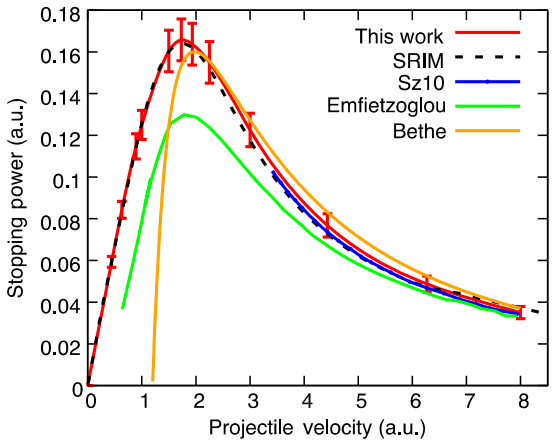

FIG. 1. Electronic stopping power curve from our first-principles simulation in comparison to the experimental data by Shimizu and co-workers [40,41] (Sz10), the SRIM [16] model, the Bethe model [44] with $I = 78$ eV recommended by the International Commission on Radiation Units and Measurement [8], and Emfietzoglou's model [10–12].

water. Our first-principles result is in excellent agreement with these two references. The peak of our calculated stopping power (i.e., the Bragg peak) is at $v = 1.73$ a.u., and the stopping power of 0.165 ± 0.010 a.u. agrees well with the SRIM model, which shows the Bragg peak at $v = 1.72$ a.u. and the stopping power of 0.165 a.u. at this velocity. For comparison, we also show the seminal Bethe model [44] with mean excitation energy parameter of $I = 78$ eV, as recommended by the International Commission on Radiation Units and Measurement [8], and one of the most recent models by Emfietzoglou and coworkers [10–12] based on perturbation theory. For the Bethe model, the Bragg peak lies around $v = 1.98$ a.u., with a corresponding stopping power of 0.160 a.u. As widely recognized, the Bethe model significantly underestimates the stopping power for low projectile velocities, and it does not obey the correct linear dependence around zero velocity [45]. At the same time, the Bethe model is remarkable in that the model correctly captures the stopping power behavior for the large projectile velocities beyond the peak velocity with only a single parameter to account for the target matter, the mean excitation energy. Emfietzoglou's model goes beyond the Bethe model, and it tends to the correct limits at both low and high velocities. However, Emfietzoglou's model shows the Bragg peak at around $v = 1.80$ a.u. with the stopping power of 0.130 a.u., which significantly underestimates the magnitude of the electronic stopping power with respect to our first-principles result.

One of the most pressing challenges is to elucidate the importance of the K-shell core-electron excitations. Widely used in radiation oncology, x- or γ-ray radiation could effectively excite deep core electrons, undergoing the Auger effect [46]. Empirical models have indicated that proton radiation does not excite K-shell core electrons appreciably for the proton velocities near the Bragg peak—only for much larger velocities [11]. In recent years, differences between x- or γ-ray and proton radiation have been examined more carefully in the radiation therapy literature [19]. However, our understanding of proton radiation is still quite limited, even for such important biological matters like liquid water. Here, we examine the extent to which the K-shell core-electron excitations play a role in the electronic stopping of protons in liquid water. In the literature, a separate K-shell contribution to stopping power is widely used, as in Emfietzoglou's model [12]. However, in addition to providing an extra channel for the energy transfer from the projectile proton, electronic excitations of K-shell core electrons also influence the valence electron excitations. This is commonly known as the "shake-up" effect [47] in the related context of x-ray absorption. In reality, it is therefore not possible to separate the electronic stopping power in terms of contributions from the valence electrons and core electrons independently, as is widely done in empirical models [11,12,48–51].

Using first-principles theory, we can quantify how much the stopping power is influenced by the presence of the K-shell core electrons by calculating the stopping power with and without the inclusion of the core electrons in our simulations, as shown in the top panel of Fig. 2. For convenience, we refer to the difference between these two stopping power curves as ΔS^{core}. The valence electron contribution indeed accounts for >99% of the stopping power for velocities of less than 1.5 a.u. However, for velocities larger than 1.5 a.u., the K-shell stopping power contribution, ΔS^{core}, starts to increase, from 0.002 a.u. (2% of the stopping power) at $v = 1.73$ a.u. to 0.012 a.u. (25% of the stopping power) at $v = 6.27$ a.u. For the highest velocity of 8.0 a.u. that we considered here, the stopping power is 28% higher when the core electrons are present. This observation differs significantly from the estimated K-shell electron contribution based on various empirical models (Emfietzoglou or Drude [11–12] and hydrogenic generalized oscillator strength [11,49,52,53]), as shown in the bottom panel of Fig. 2. For instance, Emfietzoglou's model [12] predicts that the K-shell contribution starts to become important only at much greater velocities of

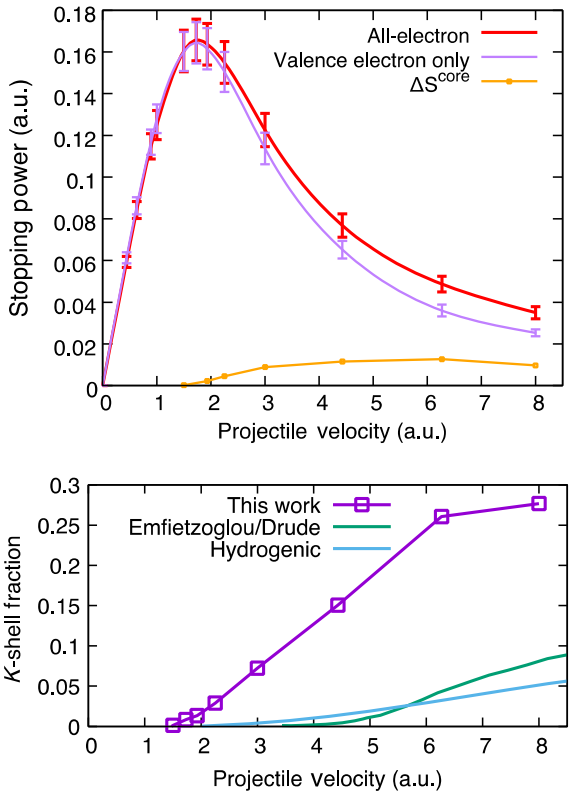

FIG. 2. (Top panel) Contribution of the K-shell (oxygen 1s electrons) excitation to electronic stopping power curve, ΔS^{core}, calculated as the difference between the all-electron and the valence-electron-only results. (Bottom panel) The fraction of the K-shell contribution to the stopping power, in comparison to the Emfietzoglou or Drude model [11,12], and the hydrogenic generalized oscillator strength model [11,49,52,53].

>3.5 a.u. [Fig. 2 (bottom panel)], and K-shell core electrons are responsible for less than 10% of the stopping power even at $v = 8.0$ a.u..

As discussed above, K-shell core-electron excitations not only provide an extra channel for the energy transfer, they also influence valence electron excitations. To quantify this shake-up effect in the electronic stopping, we calculated the summed expectation value of the Kohn-Sham (KS) Hamiltonian for all of the valence electron wave functions, $\sum\langle\varphi_i(t)\rangle|\hat{H}_{\mathrm{KS}}|\varphi_i(t)\rangle|$, in the simulations with and without the core electrons. The shake-up effect then can be quantified by obtaining the difference of these Hamiltonian expectation values for the valence electrons in the simulations with and without the K-shell core electrons. Figure 3 shows this energy difference as a function of the projectile proton displacement, averaged over all of the 64 projectile paths. The shake-up effect contribution to the stopping power is obtained by calculating this expectation value change per unit distance of the projectile proton movement. At the high proton velocity of 8.0 a.u., the shake-up effect is responsible for 36% of ΔS^{core} (i.e., 11% of the stopping power). At the Bragg peak proton velocity of 1.73 a.u., 56% of ΔS^{core} is due to the shake-up effect, but it is only <1% of the stopping power because K-shell core electrons are hardly excited at this peak velocity. For a very low velocity of 1.00 a.u., no shake-up effect is observed, and the difference between the all-electron and valence-electron-only calculations simply oscillates around zero in Fig. 3. The K-shell core-electron excitations have significant influence on the valence electron excitations at high velocities. Although having a separate correction for the core-electron excitation is convenient in modeling [12,23], it is not possible to take into account this intricate shake-up effect using such a model correction. This shake-up effect partly explains why using a separate K-shell correction underestimates the ΔS^{core} with respect to our first-principles result [see Fig. 2 (bottom panel)].

Having examined the K-shell core-electron excitations and the importance of the shake-up effect, we now turn our attention to the spatial characteristics of the excited carriers in the electronic stopping process. The time-dependent KS wave functions can be projected onto the KS eigenstates of the equilibrium electrons to obtain the excited carrier distribution [17,18]. The projection onto the occupied and unoccupied eigenstates is used to calculate the hole and excited electron populations, respectively. All of the occupied eigenstates and the unoccupied eigenstates up to 80 eV above the conduction band minimum are included in the projection, and the electronic states covered in this energy range account for greater than 95% of the total excited electrons. At the peak velocity of $v = 1.73$ a.u., the average number of holes per water molecule is 0.0933, and only 0.003% (3×10^{-6} holes) are generated in the K shell. At $v = 8.0$ a.u., the average number of holes is significantly smaller, 0.0108, but approximately 1% (1×10^{-4} holes) of the holes are generated in the K shell. Figure 4 shows the spatial distribution of the excited electrons and holes at $v = 8.0$ a.u., as a function of the distance from each projectile proton path, averaged over all of the projectile paths. A full width at half maximum (FWHM) of the distribution for the core holes is 0.76 a.u., while a noticeably broader FWHM of 4.50 a.u. is observed for the hole distribution in the valence band states. The valence hole distribution shows two notable features: a localized region that corresponds to individual water molecules along the path and the distribution tail that derives from neighboring water molecules. This tail component gives the valence hole distribution an appreciable magnitude even at distances larger than 9 a.u. On the other hand, the excited electron distribution is not so localized

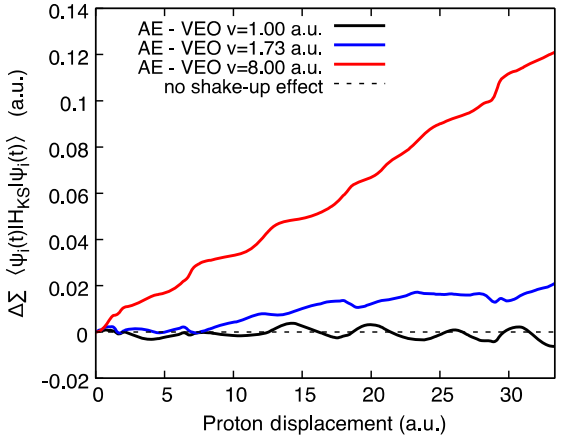

FIG. 3. Difference of the summed Hamiltonian expectation value of the valence electrons for simulations with (AE, all electrons) and without K-shell core electrons (VEO, valence electron only) at the projectile proton velocity of 1.00 a.u., 1.73 (peak), and 8.00 a.u.

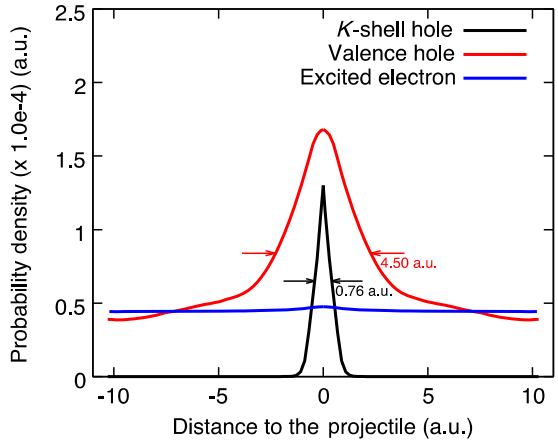

FIG. 4. Ensemble-averaged distribution of holes and excited electrons as a function of the distance from the projectile proton path at the proton velocity of 8.0 a.u. The plot is made symmetric as a guide for the eye. The arrows indicate the FWHMs of the valence hole and O 1s hole distributions.

along the projectile proton path as shown in Fig. 4, and the excited electron distribution decreases only by ∼10%, even 9 a.u. away from the path. This indicates that individual water molecules are indeed ionized along the projectile path in the electronic stopping process, which is consistent with our earlier finding [17] and also with the established notion of proton radiation as ionizing radiation. The K-shell core-electron excitations still contribute greatly to the stopping power—even when only a small proportion of the excited electrons are excited from the K-shell core states—because the core excitation energy is a few orders of magnitude greater than the valence excitation energy.

Developing a detailed understanding of the role of core-electron excitations in liquid water under proton irradiation has become important largely due to the growing use of proton beams in radiation oncology. Using nonequilibrium simulations based on real-time, time-dependent density functional theory, we accurately determined the electronic stopping power for protons in water from first principles, particularly focusing on the role of core electrons. The first-principles predicted stopping power shows significant differences from commonly used perturbation theoretic models, such as the Bethe and Emfietzoglou models [12,13,44]. The K-shell core-electron excitation from water molecules' oxygen atoms was found to be crucial in determining the electronic stopping power curve beyond its maximum, being responsible for as much as one third of the stopping power at the large proton velocity of 8.0 a.u. (the kinetic energy of 1.6 MeV). The core-electron excitation significantly influences the valence electron excitation, in addition to providing an additional channel for the energy transfer. Such a cooperative phenomenon in the excitation is often referred to as the shake-up effect [47], and this effect approximately accounts for as much as half of the contribution of the K-shell core-electron excitation to the electronic stopping power at the high proton velocity of 8.0 a.u. In the excitation process, the generated holes remain highly localized within a few angstroms around the irradiating proton path while electrons are excited away, indicative of ionizing radiation behavior. Despite their importance in contributing to the stopping power, the K-shell core electrons play a rather minor role in terms of the excitation density; only 1% of the holes are generated in the K shell even at the large velocity of 8.0 a.u. While x- and γ-ray and proton radiations are both considered to be ionizing radiation and are usually treated on the same footing [19], our work revealed that the excitation and ionization behaviors involved are distinctly different.

This work is supported by the National Science Foundation under Grants No. CHE-1565714, No. DGE-1144081, and No. OAC-1740204. An award of computer time was provided by the Innovative and Novel Computational Impact on Theory and Experiment (INCITE) program. This research used resources of the Argonne Leadership Computing Facility, which is a U.S. DOE Office of Science User Facility supported under Contract No. DE-AC02–06CH11357.

*ykanai@unc.edu

[1] C. P. Race, D. R. Mason, M. W. Finnis, W. M. C. Foulkes, A. P. Horsfield, and A. P. Sutton, The treatment of electronic excitations in atomistic models of radiation damage in metals, Rep. Prog. Phys. **73**, 116501 (2010).
[2] J. F. Ziegler, Stopping of energetic light ions in elemental matter, J. Appl. Phys. **85**, 1249 (1999).
[3] M. Scholz, Heavy ion tumour therapy, Nucl. Instrum. Methods Phys. Res., Sect. B **161**, 76 (2000).
[4] H. Stelzer, Tumor therapy with heavy ions at GSI, Nucl. Phys. **B61**, 650 (1998).
[5] E. Kamaratos, The mean excitation-energy for stopping power I, the Bragg rule, and chemical and phase effects—Application of a statistical treatment to the determination of I for chemically bound particles, Chem. Rev. **84**, 561 (1984).
[6] P. Sigmund, *Particle Penetration and Radiation Effects: General Aspects and Stopping of Swift Point Charges*, Springer Series in Solid-State Sciences Vol. 151 (Springer, New York, 2006).
[7] J. R. Sabin, J. Oddershede, R. Cabrera-Trujillo, S. P. A. Sauer, E. Deumens, and Y. Öhrn, Stopping power of molecules for fast ions, Mol. Phys. **108**, 2891 (2010).
[8] Recommended values for key data, J. Int. Comm. Radiat. Units Meas. **14**, 34 (2014).
[9] J. C. Ashley, Optical-data model for the stopping power of condensed matter for protons and antiprotons, J. Phys. Condens. Matter **3**, 2741 (1991).
[10] D. Emfietzoglou, F. A. Cucinotta, and H. Nikjoo, A complete dielectric response model for liquid water: A solution of the Bethe ridge problem, Radiat. Res. **164**, 202 (2005).
[11] D. Emfietzoglou, R. Garcia-Molina, I. Kyriakou, I. Abril, and H. Nikjoo, A dielectric response study of the electronic stopping power of liquid water for energetic protons and a new I-value for water, Phys. Med. Biol. **54**, 3451 (2009).
[12] D. Emfietzoglou, H. Nikjoo, and A. Pathak, Electronic cross sections for proton transport in liquid water based on optical-data models, Nucl. Instrum. Methods Phys. Res., Sect. B **249**, 26 (2006).
[13] R. Garcia-Molina, I. Abril, P. de Vera, I. Kyriakou, and D. Emfietzoglou, A study of the energy deposition profile of proton beams in materials of hadron therapeutic interest, Appl. Radiat. Isot. **83**, 109 (2014).
[14] D. R. Penn, Electron mean-free-path calculations using a model dielectric function, Phys. Rev. B **35**, 482 (1987).
[15] R. H. Ritchie, Energy losses by swift charged particles in the bulk and at the surface of condensed matter, Nucl. Instrum. Methods Phys. Res. **198**, 81 (1982).
[16] J. F. Ziegler, M. D. Ziegler, and J. P. Biersack, SRIM—The stopping and range of ions in matter (2010), Nucl. Instrum. Methods Phys. Res., Sect. B **268**, 1818 (2010).
[17] K. G. Reeves and Y. Kanai, Electronic excitation dynamics in liquid water under proton irradiation, Sci. Rep. **7**, 40379 (2017).
[18] K. G. Reeves, Y. Yao, and Y. Kanai, Electronic stopping power in liquid water for protons and alpha particles from first principles, Phys. Rev. B **94**, 041108 (2016).

[19] M. Durante, R. Orecchia, and J. S. Loeffler, Charged-particle therapy in cancer: Clinical uses and future perspectives, Nat. Rev. Clin. Oncol. **14**, 483 (2017).
[20] A. Schleife, E. W. Draeger, Y. Kanai, and A. A. Correa, Plane-wave pseudopotential implementation of explicit integrators for time-dependent Kohn-Sham equations in large-scale simulations, J. Chem. Phys. **137**, 22A546 (2012).
[21] A. Schleife, Y. Kanai, and A. A. Correa, Accurate atomistic first-principles calculations of electronic stopping, Phys. Rev. B **91**, 014306 (2015).
[22] D. C. Yost and Y. Kanai, Electronic stopping for protons and alpha particles from first-principles electron dynamics: The case of silicon carbide, Phys. Rev. B **94**, 115107 (2016).
[23] D. C. Yost, Y. Yao, and Y. Kanai, Examining real-time time-dependent density functional theory nonequilibrium simulations for the calculation of electronic stopping power, Phys. Rev. B **96**, 115134 (2017).
[24] J. M. Pruneda, D. Sánchez-Portal, A. Arnau, J. I. Juaristi, and E. Artacho, Electronic Stopping Power in LiF from First Principles, Phys. Rev. Lett. **99**, 235501 (2007).
[25] A. Schleife, E. W. Draeger, V. M. Anisimov, A. A. Correa, and Y. Kanai, Quantum dynamics simulation of electrons in materials on high-performance computers, Comput. Sci. Eng. **16**, 54 (2014).
[26] F. Gygi, QBOX open source code project, University of California, Davis.
[27] F. Gygi, QBOX code, QB@LL version, Lawrence Livermore National Laboratory.
[28] D. R. Hamann, Optimized norm-conserving Vanderbilt pseudopotentials, Phys. Rev. B **88**, 085117 (2013).
[29] M. Schlipf and F. Gygi, Optimization algorithm for the generation of ONCV pseudopotentials, Comput. Phys. Commun. **196**, 36 (2015).
[30] See Supplemental Material at http://link.aps.org/supplemental/10.1103/PhysRevLett.123.066401, which includes Refs. [31–33], for computational details and a comparison to earlier RTTDDFT results and empirical and analytical models.
[31] A. Nilsson, D. Nordlund, I. Waluyo, N. Huang, H. Ogasawara, S. Kaya, U. Bergmann, L. Å. Näslund, H. Öström, P. Wernet, K. J. Andersson, T. Schiros, and L. G. M. Pettersson, X-ray absorption spectroscopy and x-ray Raman scattering of water and ice; an experimental view, J. Electron Spectrosc. Relat. Phenom. **177**, 99 (2010).
[32] C. Fonseca Guerra, J. W. Handgraaf, E. J. Baerends, and F. M. Bickelhaupt, Voronoi deformation density (VDD) charges: Assessment of the Mulliken, Bader, Hirshfeld, Weinhold, and VDD methods for charge analysis, J. Comput. Chem. **25**, 189 (2004).
[33] G. Schiwietz and P. Grande, Improved charge-state formulas, Nucl. Instrum. Methods Phys. Res., Sect. B **175**, 125 (2001).
[34] J. P. Perdew, K. Burke, and M. Ernzerhof, Generalized Gradient Approximation Made Simple, Phys. Rev. Lett. **77**, 3865 (1996).
[35] J. Sun, R. C. Remsing, Y. Zhang, Z. Sun, A. Ruzsinszky, H. Peng, Z. Yang, A. Paul, U. Waghmare, X. Wu, M. L. Klein, and J. P. Perdew, Accurate first-principles structures and energies of diversely bonded systems from an efficient density functional, Nat. Chem. **8**, 831 (2016).
[36] J. Sun, A. Ruzsinszky, and J. P. Perdew, Strongly Constrained and Appropriately Normed Semilocal Density Functional, Phys. Rev. Lett. **115**, 036402 (2015).
[37] Y. Yao and Y. Kanai, Plane-wave pseudopotential implementation and performance of SCAN meta-GGA exchange-correlation functional for extended systems, J. Chem. Phys. **146**, 224105 (2017).
[38] H. J. C. Berendsen, J. R. Grigera, and T. P. Straatsma, The missing term in effective pair potentials, J. Phys. Chem. **91**, 6269 (1987).
[39] R. Ullah, E. Artacho, and A. A. Correa, Core Electrons in the Electronic Stopping of Heavy Ions, Phys. Rev. Lett. **121**, 116401 (2018).
[40] M. Shimizu, T. Hayakawa, M. Kaneda, H. Tsuchida, and A. Itoh, Stopping cross-sections of liquid water for 0.3–2.0 MeV protons, Vacuum **84**, 1002 (2010).
[41] M. Shimizu, M. Kaneda, T. Hayakawa, H. Tsuchida, and A. Itoh, Stopping cross sections of liquid water for MeV energy protons, Nucl. Instrum. Methods Phys. Res., Sect. B **267**, 2667 (2009).
[42] R. Garcia-Molina, I. Abril, P. de Vera, and H. Paul, Comments on recent measurements of the stopping power of liquid water, Nucl. Instrum. Methods Phys. Res., Sect. B **299**, 51 (2013).
[43] J. Lindhard, V. Nielsen, M. Scharff, and P. Thomsen, Integral equations governing radiation effects, Mat. Fys. Medd. K. Dan. Vidensk. Selsk **33**, No. 10 (1963).
[44] H. Bethe, Theory of the passage of fast corpuscular rays through matter, Ann. Phys. (Berlin) **397**, 325 (1930).
[45] S. P. Ahlen, Theoretical and experimental aspects of the energy loss of relativistic heavily ionizing particles. Rev. Mod. Phys. **52**, 121 (1980).
[46] A. Yokoya and T. Ito, Photon-induced Auger effect in biological systems: A review, Int. J. Radiat. Biol. **93**, 743 (2017).
[47] P. Persson, S. Lunell, A. Szöke, B. Ziaja, and J. Hajdu, Shake-up and shake-off excitations with associated electron losses in x-ray studies of proteins, Protein Sci. **10**, 2480 (2001).
[48] R. Garcia-Molina, I. Abril, S. Heredia-Avalos, I. Kyriakou, and D. Emfietzoglou, A combined molecular dynamics and Monte Carlo simulation of the spatial distribution of energy deposition by proton beams in liquid water, Phys. Med. Biol. **56**, 6475 (2011).
[49] M. Dingfelder, M. Inokuti, and H. G. Paretzke, Inelastic-collision cross sections of liquid water for interactions of energetic protons, Radiat. Phys. Chem. **59**, 255 (2000).
[50] H. Date, K. Sutherland, T. Hayashi, Y. Matsuzaki, and Y. Kiyanagi, Inelastic collision processes of low-energy protons in liquid water, Radiat. Phys. Chem. **75**, 179 (2006).
[51] M. Bernal and J. Liendo, Inelastic-collision cross sections for the interactions of totally stripped H, He and C ions with

liquid water, Nucl. Instrum. Methods Phys. Res., Sect. B **262**, 1 (2007).

[52] S. Heredia-Avalos, R. Garcia-Molina, J. M. Fernández-Varea, and I. Abril, Calculated energy loss of swift He, Li, B, and N ions in SiO_2, Al_2O_3, and ZrO_2, Phys. Rev. A **72**, 052902 (2005).

[53] R. Garcia-Molina, I. Abril, C. D. Denton, S. Heredia-Avalos, I. Kyriakou, and D. Emfietzoglou, Calculated depth-dose distributions for H+ and He+ beams in liquid water, Nucl. Instrum. Methods Phys. Res., Sect. B **267**, 2647 (2009).